

# Electrostatic forces involved in orienting *Anabaena* ferredoxin during binding to *Anabaena* ferredoxin:NADP<sup>+</sup> reductase: Site-specific mutagenesis, transient kinetic measurements, and electrostatic surface potentials

JOHN K. HURLEY,<sup>1</sup> JAMES T. HAZZARD,<sup>1</sup> MARTA MARTÍNEZ-JÚLVEZ,<sup>2</sup> MILAGROS MEDINA,<sup>2</sup> CARLOS GÓMEZ-MORENO,<sup>2</sup> AND GORDON TOLLIN<sup>1</sup>

<sup>1</sup>Department of Biochemistry, University of Arizona, Tucson, Arizona 85721

<sup>2</sup>Departamento de Bioquímica y Biología Molecular y Celular, Universidad de Zaragoza, E50009, Zaragoza, Spain

(RECEIVED January 19, 1999; ACCEPTED April 19, 1999)

## Abstract

Transient absorbance measurements following laser flash photolysis have been used to measure the rate constants for electron transfer (et) from reduced *Anabaena* ferredoxin (Fd) to wild-type and seven site-specific charge-reversal mutants of *Anabaena* ferredoxin:NADP<sup>+</sup> reductase (FNR). These mutations have been designed to probe the importance of specific positively charged amino acid residues on the surface of the FNR molecule near the exposed edge of the FAD cofactor in the protein–protein interaction during et with Fd. The mutant proteins fall into two groups: overall, the K75E, R16E, and K72E mutants are most severely impaired in et, and the K138E, R264E, K290E, and K294E mutants are impaired to a lesser extent, although the degree of impairment varies with ionic strength. Binding constants for complex formation between the oxidized proteins and for the transient et complexes show that the severity of the alterations in et kinetics for the mutants correlate with decreased stabilities of the protein–protein complexes. Those mutated residues, which show the largest effects, are located in a region of the protein in which positive charge predominates, and charge reversals have large effects on the calculated local surface electrostatic potential. In contrast, K138, R264, K290, and K294 are located within or close to regions of intense negative potential, and therefore the introduction of additional negative charges have considerably smaller effects on the calculated surface potential. We attribute the relative changes in et kinetics and complex binding constants for these mutants to these characteristics of the surface charge distribution in FNR and conclude that the positively charged region of the FNR surface located in the vicinity of K75, R16, and K72 is especially important in the binding and orientation of Fd during electron transfer.

**Keywords:** electron transfer proteins; laser flash photolysis; protein–protein complexes; role of basic residues

To gain insight into the structural factors that lead to binding and subsequent electron transfer (et) between redox proteins, we have used the 36 kDa form of *Anabaena* 7119 ferredoxin:NADP<sup>+</sup> reductase (FNR) and *Anabaena* 7120 vegetative cell ferredoxin (Fd) as a paradigm for this process. This system is ideal in that both proteins have been cloned and overexpressed in *Escherichia coli* (Alam et al., 1986; Böhme & Haselkorn, 1989; Fillat et al., 1990, 1994; Gómez-Moreno et al., 1995), thereby allowing site-specific

mutagenesis, and the three-dimensional structures of both proteins have been solved to high resolution (Rypniewski et al., 1991; Holden et al., 1994; Serre et al., 1996). Fd is an 11 kDa acidic protein having a single [2Fe-2S] cluster as its prosthetic group. Although it is involved in a number of different metabolic pathways (Knaff & Hirasawa, 1991; Knaff, 1996), its interaction with FNR occurs in the photosynthetic electron transport chain where it is the terminal electron acceptor from Photosystem I. Subsequent to this, it transfers two electrons (in one-electron steps) to FNR, which catalyzes the reduction of NADP<sup>+</sup> to NADPH as depicted in Equation 1:



FNR is a basic protein containing one noncovalently bound FAD cofactor. Fd and FNR react in a (minimal) two-step mechanism

Reprint requests to: Gordon Tollin, Department of Biochemistry, University of Arizona, Tucson, Arizona 85721; e-mail: gtollin@u.arizona.edu.

**Abbreviations:** dRf, 5-deazariboflavin; dRfH•, dRf semiquinone; EDTA, ethylenediaminetetraacetic acid; et, electron transfer; FAD, flavin adenine dinucleotide; Fd, ferredoxin; Fd<sub>ox</sub>, oxidized Fd; Fd<sub>red</sub>, reduced Fd; FNR, ferredoxin:NADP<sup>+</sup> reductase; FNR<sub>ox</sub>, oxidized FNR; FNR<sub>red</sub>, FNR semiquinone; wt, wild-type.

involving complex formation followed by et, as depicted in Equation 2:



where  $K_d$  and  $k_{et}$  represent the dissociation constant and et rate constant, respectively, for the transient  $\text{Fd}_{\text{red}}:\text{FNR}_{\text{ox}}$  complex. Included in  $k_{et}$  are factors such as protein structural rearrangements and changes in hydration of the proteins occurring upon complexation, as well as the intrinsic et rate constant.

We have been using a combination of site-specific mutagenesis and time-resolved absorbance measurements to determine the effects of amino acid substitutions at selected sites in Fd and FNR on the et reaction between these two proteins. Most recently, we have been altering residues in FNR, and we have shown that E301 (Medina et al., 1998) and K75 (Martínez-Júlvez et al., 1998) are critical for et with Fd. Mutation of the residue homologous to E301 in spinach FNR (E312) has recently been shown to also impair the et process with spinach Fd (Aliverti et al., 1998). Both of these residues are located on the surface of FNR close to the exposed edge of the FAD prosthetic group, which lies in a depression likely to be the Fd binding site. In the case of E301, it was concluded (Medina et al., 1998) that the side-chain carboxylate of this residue stabilizes the transition state for et between the FAD and the [2Fe-2S] cluster. For K75, we have shown that a positive charge is required at this position for rapid et with Fd and that it was protein-protein complex stability that was principally affected by mutation. A recent steady-state kinetic study (Schmitz et al., 1998) confirmed the critical nature of K75 and also investigated the importance of a number of other positively charged residues of FNR in the et interaction with Fd. Selection of these basic residues for mutation was based on insights gained from the structure determination of *Anabaena* 7119 FNR (Serre et al., 1996), from cross-linking and chemical modification studies on the spinach (Zanetti et al., 1988; Zanetti & Aliverti, 1991; De Pascalis et al., 1993; Jelesarov et al., 1993) and *Anabaena* (Medina et al., 1992a, 1992b) proteins, from steady-state kinetic measurements on the *Anabaena* proteins (Gómez-Moreno et al., 1995), and from a mutagenesis study with the spinach proteins (Aliverti et al., 1994). In addition, further information concerning the possible importance of these residues has been obtained from docking models of spinach FNR with *Spirulina platensis* (Karplus, 1991; Karplus et al., 1991) and *Aphanathece sacrum* Fds (Karplus & Bruns, 1994), and a model (De Pascalis et al., 1993) in which the spinach Fd sequence was fit to the structure of the Fd from *A. sacrum* (Fukuyama et al., 1995).

That electrostatic interactions are involved in the Fd/FNR interaction has been known for some time (Foust et al., 1969), and much of the research involving the interaction of Fd with FNR was based on this premise. Molecular dipole moments have been calculated for spinach Fd (De Pascalis et al., 1993) and spinach FNR molecules (Jelesarov et al., 1993), and it has been suggested that the molecules are initially "steered toward each other" via complementary interactions of these dipoles (De Pascalis et al., 1993), which bring the molecules into approximately the proper orientation for formation of an efficient et complex. Interactions of basic residues on FNR and acidic residues on Fd may then help in the attainment of the optimal orientation (De Pascalis et al., 1993). It was also inferred that such salt links "may not make strong contributions to binding energy at physiological ionic strength and may not be essential for electrostatic interaction" (De Pascalis

et al., 1993). However, several reports from our laboratories have shown that there is a high level of specificity involving charged residues at the protein:protein interface, even at 100 mM ionic strength (Hurley et al., 1993, 1995, 1997a). It is also important to note that there is evidence for the involvement of hydrophobic interactions in the formation of a productive et complex (Hurley et al., 1993, 1996; Jelesarov & Bosshard, 1994).

The present studies were designed to extend our knowledge of the importance of positively charged residues in FNR in the protein-protein interactions leading to et by comparing the transient kinetic and Fd binding properties of the charge-reversal mutant K75E with similar mutations at the other basic residues previously investigated by steady-state kinetic methods. Consistent with the latter results (Schmitz et al., 1998), the transient kinetic measurements described herein demonstrate that the FNR mutants R16E, K72E, and K75E have substantially altered et kinetics with  $\text{Fd}_{\text{red}}$ , with K75E being the most severely impaired mutant, whereas the K138E, R264E, K290E, and K294E mutants are considerably less impaired (see Fig. 1 for the location of these highly conserved residues on the FNR surface). The binding constants for the corresponding protein-protein complexes are shown to correlate with these kinetic properties. Calculations of surface electrostatic potential maps for wt and computer-generated FNR mutants have provided additional insights into these effects.

## Materials and methods

### Oligonucleotide-directed mutagenesis

Mutants of recombinant *Anabaena* PCC 7119 FNR were produced using as a template a construct of the *petH* gene, which had been previously cloned into the expression vector pTrc99a (Fillat et al., 1994). Mutations were obtained using the Transformer™ site-directed mutagenesis kit from CLONTECH (Palo Alto, California) in combination with the synthetic oligonucleotide: 5' GGAGCAT

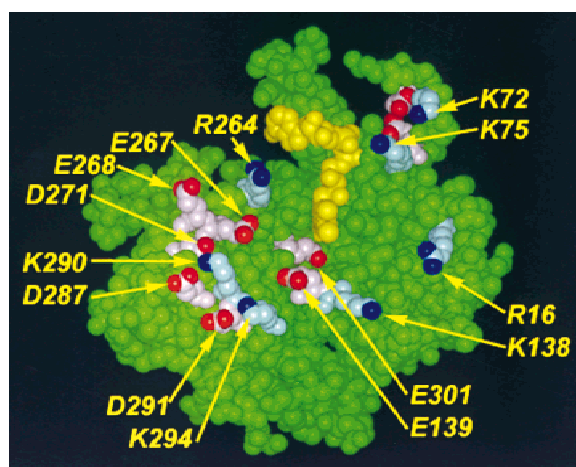


**Fig. 1.** CPK representation of wt FNR. The basic side chains that were mutated are shown in light blue (nitrogen atoms in dark blue). Pertinent acidic residues are shown in light red (carboxylate oxygens in dark red). The FAD cofactor is shown in yellow. This model was generated using INSIGHT II (Molecular Simulations, Inc., San Diego, California). The coordinates are from the Brookhaven Protein Data Bank (file code = 1QUE).

TGGG“CTC”GTAAAGATTAACAGG 3' for R16E, 5' TCCGGC T“C”GCCGTCTTGTC 3' for K72E, 5' GAGTCTCAATT“C” TTCCGGCTTGCC 3' for K75E, 5' CAGACATTTCTT“C”ACC CACAGGCC 3' for K138E, 5' CTCTTCCATACC“CTC”CAA ACCACAGATG 3' for R264E, 5' CTTGAGGTCTT“C”TTGGT AATCAC 3' for K290E, 5' GCGACCAGCTT“C”TTGAGGTC 3' for K294E, and the trans oligo NdeI/Sac II 5' AGTGCACCA TCCGCGGTGTGA 3'.

Mutations were verified by DNA sequence analysis. The constructs containing the mutated FNR gene were used to transform the *E. coli* PC 0225 strain (Gómez-Moreno et al., 1995).

#### Protein preparation

Wt Fd was prepared as described previously (Hurley et al., 1993). *Anabaena* PCC 7119 FNR wt and mutants were purified from IPTG-induced cultures as previously described (Gómez-Moreno et al., 1995; Medina et al., 1998). UV-visible spectra and SDS-PAGE electrophoresis were used as purity criteria.

#### Laser flash photolysis/transient absorbance measurements

The laser flash photolysis system and associated optics have been described previously (Bhattacharyya et al., 1983; Hurley et al., 1996; Przysiecki et al., 1985). The photochemical mechanism by which 5-deazariboflavin (dRf) initiates protein-protein et has also been described (Tollin & Hazzard, 1991; Tollin et al., 1993; Tollin, 1995). Briefly, a N<sub>2</sub> laser (Photochemical Research Associates (PRA), London, Ontario, Canada) was used to pump a dye laser (BBQ 2A368 dye, 396 nm wavelength maximum; PRA), which was focused onto the sample cell. In addition to protein, the sample cell also contained 100 μM dRf and 1 mM EDTA in 4 mM potassium phosphate buffer (pH 7.0). Samples were deaerated by bubbling with H<sub>2</sub>O-saturated O<sub>2</sub>-free Ar for 1 h prior to addition of microliter volumes of protein. The ionic strength was adjusted using aliquots of 5 M NaCl. Where necessary, Ar was blown over the surface of the sample to remove traces of O<sub>2</sub> introduced into the sample cell during protein or salt addition. Experiments were performed at room temperature.

The triplet state of dRf, formed by the laser flash, abstracts a hydrogen atom from EDTA producing the highly reducing dRf semiquinone radical (dRfH•) in less than 1 μs. The dRfH• radical, in competition with its own disproportionation, reduces Fd, which is present in large excess over the concentration of dRfH• produced by the laser flash, thereby ensuring pseudo-first-order reaction conditions. Upon subsequent additions of FNR, et from Fd<sub>red</sub> to FNR<sub>ox</sub> can be observed. Rate constants were measured using absorbance measurements at 600 nm, where the production of the FNR semiquinone is observed. Data taken at 507 nm, which monitors the oxidation state of the Fd, gave results that were the same, within experimental error, as those obtained at 600 nm. Generally, data from 3–10 laser flashes were averaged. Data were fit to mono-exponential curves using the curve-fitting routine Kinfit (OLIS, Inc., Bogart, Georgia). Examples of transient decay curves similar to those observed in the present set of experiments have been published previously (Hurley et al., 1997a, 1997b).

#### Binding constant measurements

The dissociation constants between oxidized Fd and oxidized wt and mutant FNRs were measured by differential absorption mea-

surements as described previously (Sancho & Gómez-Moreno, 1991). The binding constants for the transient Fd<sub>red</sub>:FNR<sub>ox</sub> complex were determined by fitting the kinetic data to the exact solution of the differential equation describing the mechanism (Simonsen et al., 1982; Simonsen & Tollin, 1983). The electron transfer rate constant  $k_{et}$ , which includes contributions from structural rearrangements of the proteins and changes in hydration of the proteins, as well as the electron transfer step itself, is also determined by this analysis.

#### CPK model and electrostatic potential surface map of FNR

The computer program INSIGHT II (Molecular Simulations, Inc., San Diego, California) was used to generate the CPK model of FNR. Structures of the mutant FNRs were made by replacement of the appropriate amino acid using this software package. The resulting structures were energy minimized, with the constraint that only the replaced amino acid side chain could move, using HOMOLGY (Molecular Simulations, Inc.). Electrostatic potentials for all structures were calculated using DELPHI (Molecular Simulations, Inc.), with an ionic strength of 12 mM. Mapping of the electrostatic potential onto the molecular surface of the protein (Nicholls et al., 1991) was performed using GRASP (Molecular Simulations, Inc.), with a potential range of -15 to +15 eV. Coordinates from the crystal structure determined by Serre et al. (1996) were obtained from the Brookhaven Protein Data Bank (file code = 1QUE).

## Results and discussion

#### Transient kinetics

At 12 mM ionic strength, the rate constants for the reduction of wt and mutant FNRs by laser-generated dRfH• ranged from 1.4 to  $3.5 \times 10^8 \text{ M}^{-1} \text{ s}^{-1}$  (data not shown). This is typical of the values we have obtained previously for wt and other FNR mutants (Martínez-Júlvez et al., 1998; Medina et al., 1998). We take this as an indication that the FAD prosthetic group in these mutant forms of FNR is as accessible and has comparable redox activity to the wt protein.

We have previously (Martínez-Júlvez et al., 1998; Medina et al., 1998) used measurements of the FNR<sub>ox</sub> concentration dependence of the extent of reoxidation of Fd<sub>red</sub> to estimate the redox potential for the oxidized FNR/semiquinone FNR couple ( $E_1^{\circ}$ ) in FNR mutants, a quantity that is quite difficult to obtain electrochemically. For the mutants investigated herein, we found that the concentrations of R16E, K72E, R264E, K290E, and K294E required to completely reoxidize Fd<sub>red</sub> in a laser flash photolysis experiment were closely similar to that found with wt FNR, indicating that  $E_1^{\circ}$  for these mutants is comparable to that of the wt protein (-331 mV vs. NHE; Hurley et al., 1997a). In contrast, approximately twice as much K75E and K138E were required to completely oxidize Fd<sub>red</sub>, indicating that the  $E_1^{\circ}$  values for these mutants are approximately 20 mV more negative than for wt FNR (i.e.,  $\approx -351 \text{ mV}$ ). This small change in reduction potential for K75E cannot account for the large decreases in et reactivity with Fd<sub>red</sub> observed for this mutant (see below). Furthermore, despite this change, K138E reacts much like wt FNR (see below). Thus, we conclude that factors other than redox potential are involved in altering the et behavior of these mutants.

The  $k_{obs}$  values for the reduction of wt FNR and the seven FNR mutants by  $Fd_{red}$  showed a linear dependence on FNR concentration at an ionic strength of 12 mM (data not shown). We have corrected these data for the concentration of preformed complex, which we have previously shown to be unreactive toward  $Fd_{red}$  (Hurley et al., 1996), using the measured binding constants for the oxidized proteins as listed in Table 1. After such correction, all of the mutants except R16E, K72E, and K75E (data for the latter protein could not be corrected because its binding affinity was too small to be measurable) showed nonlinear concentration dependencies (Fig. 2), as has been observed previously (Hurley et al., 1996). Such behavior allows the calculation of  $k_{et}$  and of the  $K_d$  value for the transient  $Fd_{red}:FNR_{ox}$  complex (Table 1; see Materials and methods). As shown in Table 1, at 12 mM ionic strength the  $k_{et}$  values, as well as the second order rate constants estimated from the nonlinear concentration plots, for the K138E, R264E, K290E, and K294E mutants were quite similar to those for wt FNR. The  $K_d^{red}$  values for the transient  $Fd_{red}:FNR_{ox}$  complexes for these four mutants were also quite similar to that of wt FNR, although the  $K_d^{ox}$  values (for the complexes between the oxidized proteins) were significantly larger. It is interesting to note that upon reduction of Fd, wt  $FNR_{ox}$  forms a weaker complex than that formed with  $Fd_{ox}$ . In contrast to this, the K138E, R264E, K290E, and K294E mutants form tighter complexes with  $Fd_{red}$  than with  $Fd_{ox}$ , with affinities closely similar to the wt protein. These observations imply that significant structural differences exist in the  $Fd_{ox}$  complexes with the mutant FNRs compared to wt FNR, presumably caused by the charge reversals, and that these structural differences are minimized when the complex is formed with  $Fd_{red}$ . Without additional three-dimensional structural information, it is difficult to predict what these differences might be.

**Table 1.** Kinetic parameters for electron transfer from reduced Fd to wt and mutant FNRs and dissociation constants for the  $Fd_{ox}:FNR_{ox}$  complexes at 12 mM ionic strength<sup>a</sup>

FNR/mutant	$K_d^{ox}$ ( $\mu M$ ) <sup>b</sup>	$k \times 10^{-8}$ ( $M^{-1} s^{-1}$ ) <sup>c</sup>	$K_d^{red}$ ( $\mu M$ ) <sup>d,e</sup>	$k_{et}$ ( $s^{-1}$ ) <sup>e</sup>
wt	$0.3 \pm 0.1^f$	$6.9 \pm 0.3$	$2.2 \pm 0.3^f$	$3,600 \pm 400^f$
K138E	$4.1 \pm 0.8$	$9.8 \pm 0.7$	$1.8 \pm 0.2$	$3,700 \pm 400$
R264E	$3.3 \pm 1.1$	$13.0 \pm 0.2$	$1.3 \pm 0.2$	$3,800 \pm 500$
K290E	$9.2 \pm 2.4$	$8.9 \pm 1.2$	$1.9 \pm 0.3$	$3,500 \pm 600$
K294E	$7.2 \pm 1.3$	$8.9 \pm 0.7$	$2.9 \pm 0.2$	$4,800 \pm 300$
R16E	$120 \pm 20$	$0.8 \pm 0.1$	g	—
K72E	$50 \pm 15$	$1.6 \pm 0.5$	g	—
K75E	nd <sup>h</sup>	$0.045 \pm 0.003$	g	—

<sup>a</sup>Solutions contained 100  $\mu M$  dRf, 1 mM EDTA in 4 mM potassium phosphate buffer, pH 7.0. For the kinetic experiments, FNR was titrated into a solution of either 30 or 40  $\mu M$  Fd.

<sup>b</sup> $K_d^{ox}$  is for the  $Fd_{ox}:FNR_{ox}$  complex.

<sup>c</sup>Second order rate constants were estimated from the initial slopes of  $k_{obs}$  vs. [FNR] curves, except for R16E, K72E, and K75E, which were calculated from the linear plots shown in Figure 2C.

<sup>d</sup> $K_d^{red}$  is for the transient  $Fd_{red}:FNR_{ox}$  complex.

<sup>e</sup>Values were obtained from the kinetic data, after correction for the concentration of pre-formed complex, as described in Materials and methods.

<sup>f</sup>Data are taken from Hurley et al. (1996).

<sup>g</sup>Not determined; saturation kinetics were not obtained, presumably because complex formation was too weak.

<sup>h</sup>Not determined; binding, or the spectral perturbation due to binding, was too weak to be measured for this mutant.

For the R16E, K72E, and K75E mutants, the measured second order rate constants ( $k$ ) are given in Table 1. These can be compared with the second order rate constants estimated for the wt and the other mutants, which are also included in Table 1. As is evident, the  $k$  values fall into two groups reflecting the relative et reactivities, with those for K138E, R264E, K290E, and K294E being similar in magnitude to that of wt FNR, and K75E, R16E, and K72E being significantly smaller than the wt value, with K75E being the most severely affected. It should be noted that these second order rate constants include contributions from both the complex formation and et steps (i.e.,  $K_d$  and  $k_{et}$ ). As noted above, all of the mutants except K75E and K138E have reduction potentials ( $E_1^\circ$ ) similar to wt FNR, with the latter mutants having reduction potentials approximately 20 mV more negative than wt FNR (see above). Thus, reduction potential cannot account for the decreased et reactivity of the R16, K72, and K75 mutants. However, the clear correlation found between the  $K_d$  values for the complexes formed between the oxidized proteins and the second order rate constants given in Table 1 indicates that impaired binding to Fd is the cause of the lowered reactivity of the R16E, K72E, and K75E FNR mutants at 12 mM ionic strength.

The ionic strength dependencies of the  $k_{obs}$  values for these mutants (determined at a fixed concentration of both proteins) are given in Figure 3. Although all of the mutants are impaired relative to wt FNR in the physiological ionic strength range ( $\approx 150$  mM;  $\mu^{1/2} = 0.4$ ), the decrease in reactivity is again largest for the K75E, R16E, and K72E mutants, with the K75E mutant being the most severely affected. It is also noteworthy that these effects are apparently reversed for most of the mutants (except for K75E) at the lowest ionic strengths ( $\approx 12$  mM;  $\mu^{1/2} = 0.1-0.2$ ). This is due to the fact that the wt FNR reaction with  $Fd_{red}$  is highly hindered at low ionic strengths, as a consequence of formation of a tight but nonproductive complex between the oxidized proteins resulting in a strongly biphasic ionic strength dependency of the observed rate constants (Hurley et al., 1996). When such complex formation is corrected for, as is done in Table 1, the true relative reactivities for all of the mutants at low ionic strengths can be assessed.

As shown in Figure 3, only the wt FNR had a clearly biphasic ionic strength profile (with the possible exception of the R264E mutant). Increasing the salt concentration masks this effect by weakening the electrostatic interactions occurring between the proteins. These results suggest that the charge reversals in all of the mutants sufficiently altered the electrostatic contributions to complex formation so as to minimize this behavior, i.e., complexes were either more reactive at low ionic strengths than for wt FNR, or it required lower salt concentrations to disrupt them, or both.

The FNR concentration dependencies of the et reactions from  $Fd_{red}$  to oxidized wt and mutant FNRs were also determined at the more physiologically relevant ionic strength value of 100 mM (Fig. 4), where electrostatic effects are less important. Note that, as does wt FNR, the R264E, R290E, K72E, and R16E mutants showed nonlinear behavior from which the  $k_{et}$  values given in Table 2 were determined (these data have not been corrected for pre-formed complex; we have previously shown (Hurley et al., 1996) that although this correction has negligible effects on  $k_{et}$ , it can significantly affect  $K_d$  values, which have not been included in Table 2 for this reason). Nonlinear plots were not obtained with the K75E, K138E, and K294E mutants, and thus  $k_{et}$  could not be determined. The second order rate constants derived from the linear plots for these three mutants (Fig. 4B) are also listed in Table 2 and, for comparison, second order rate constants have been estimated for

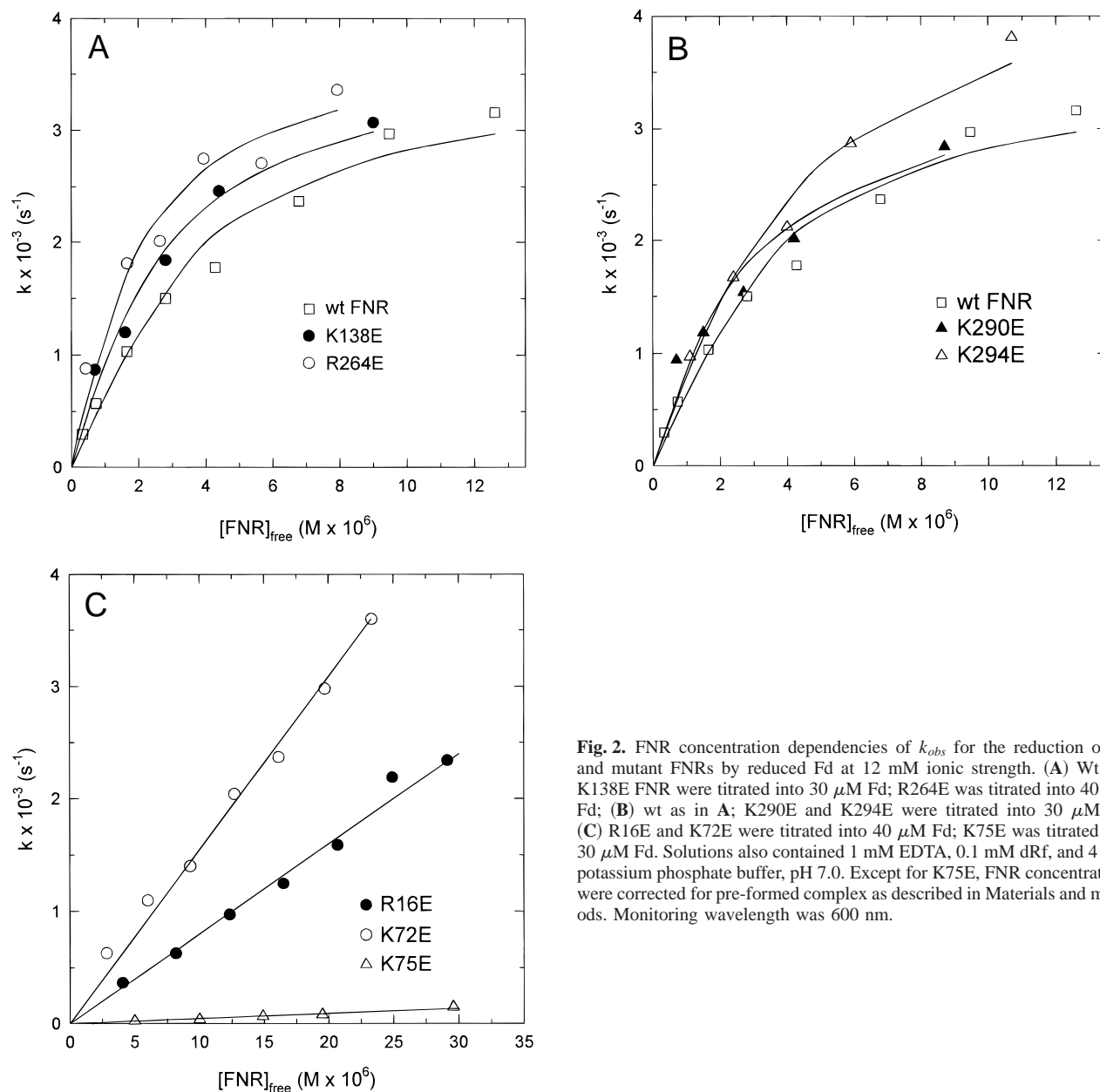


**Fig. 2.** FNR concentration dependencies of  $k_{obs}$  for the reduction of wt and mutant FNRs by reduced Fd at 12 mM ionic strength. (A) Wt and K138E FNR were titrated into 30  $\mu\text{M}$  Fd; R264E was titrated into 40  $\mu\text{M}$  Fd; (B) wt as in A; K290E and K294E were titrated into 30  $\mu\text{M}$  Fd; (C) R16E and K72E were titrated into 40  $\mu\text{M}$  Fd; K75E was titrated into 30  $\mu\text{M}$  Fd. Solutions also contained 1 mM EDTA, 0.1 mM dRf, and 4 mM potassium phosphate buffer, pH 7.0. Except for K75E, FNR concentrations were corrected for pre-formed complex as described in Materials and methods. Monitoring wavelength was 600 nm.

the other four mutants. These are also listed in Table 2. As was observed for the 12 mM ionic strength data, the same two groupings of mutants is again observed, with K75E being the most significantly altered, although all of the charge-reversal mutants are significantly hindered in et with Fd at this ionic strength. Although we have not directly determined  $K_d$  values for the oxidized proteins at 100 mM ionic strength, it is reasonable to presume that weakened binding is responsible for the lack of nonlinear behavior in the et kinetic experiments.

Using the X-ray coordinates for the wt protein, we find no correlation between the et reactivity of a given mutant and the distance of the mutated residue from the dimethylbenzene ring of the FAD cofactor (Table 3). Thus, the closest mutated residue to the flavin, R264, is not hindered in et at 12 mM ionic strength and is only moderately affected at 100 mM ionic strength, whereas the

two most hindered mutants (at both ionic strengths), R16E and K75E, are at approximately the same distance as the relatively uninhibited mutant K138E.

#### Electrostatic surface potentials

Figure 5 shows a model of the front surfaces of wt and mutant FNRs with the calculated electrostatic potentials, at 12 mM ionic strength, mapped onto the protein surfaces (Fig. 1 shows the location of the exposed edge of the FAD cofactor and the mutated residues). Several features of the structure are worth noting (also see Table 3). The flavin ring lies in a shallow depression with the methyl groups of the dimethylbenzene ring pointing out toward the viewer at approximately the center of the model, just

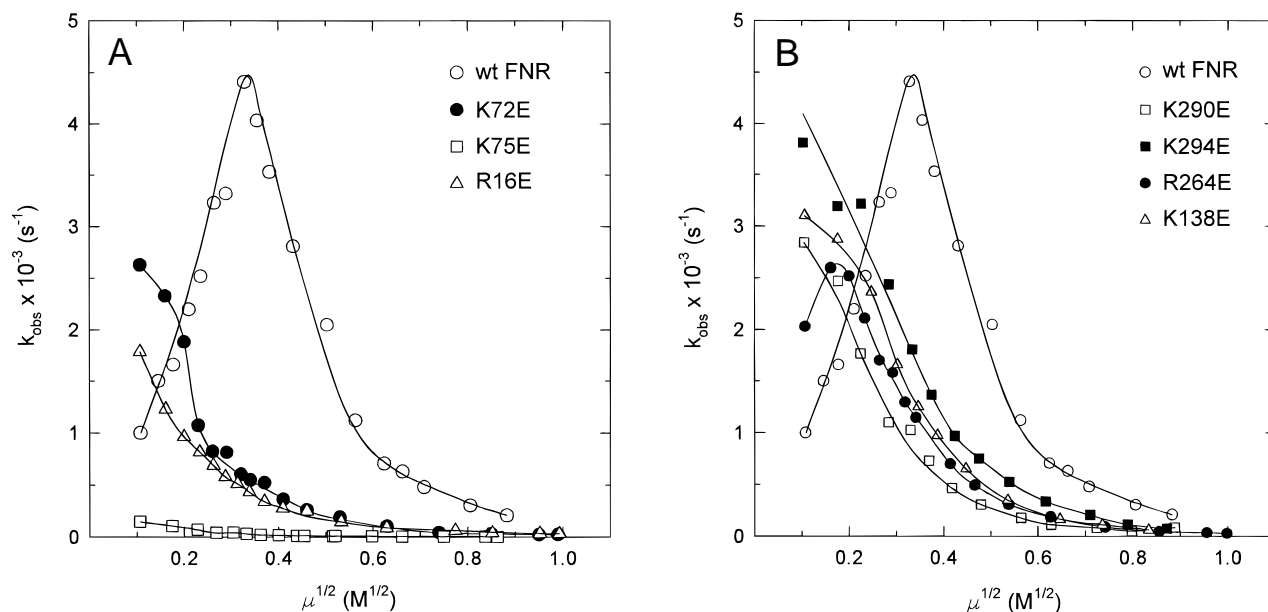


**Fig. 3.** Ionic strength dependencies for the reduction of wt and mutant FNRs by reduced Fd. The  $k_{obs}$  values for the K72E and R16E curves in **A** and for R264E in **B** have been normalized to 30  $\mu\text{M}$  FNR. Actual protein concentrations were (A) 40  $\mu\text{M}$  Fd + 30  $\mu\text{M}$  wt FNR; 38  $\mu\text{M}$  Fd + 40  $\mu\text{M}$  K72E; 39  $\mu\text{M}$  Fd + 40  $\mu\text{M}$  R16E; (B) wt same as in A; 30  $\mu\text{M}$  Fd + 30  $\mu\text{M}$  K138E; 40  $\mu\text{M}$  Fd + 40  $\mu\text{M}$  R264E; the K290E and K294E experiments contained 30  $\mu\text{M}$  Fd and 30  $\mu\text{M}$  mutant FNR. Samples also contained 4 mM potassium phosphate buffer (pH 7.0), 1 mM EDTA and 100  $\mu\text{M}$  5-deazariboflavin. The ionic strength was adjusted using 5 M NaCl. The monitoring wavelength was 600 nm.

above a region of intense negative charge (due to E301 and E139; see Fig. 1). Above the FAD pocket are two projections, one of which contains two mutation sites (K72E and K75E). Also located near K72 and K75 are two acidic residues, D68

and E74 (shown in Fig. 1, but not labeled), which, because of the orientation of the side chains, are not close enough to have salt bridges to either of these two lysines. R16 and K138 are not charged-paired with any acidic residue, lying instead within a

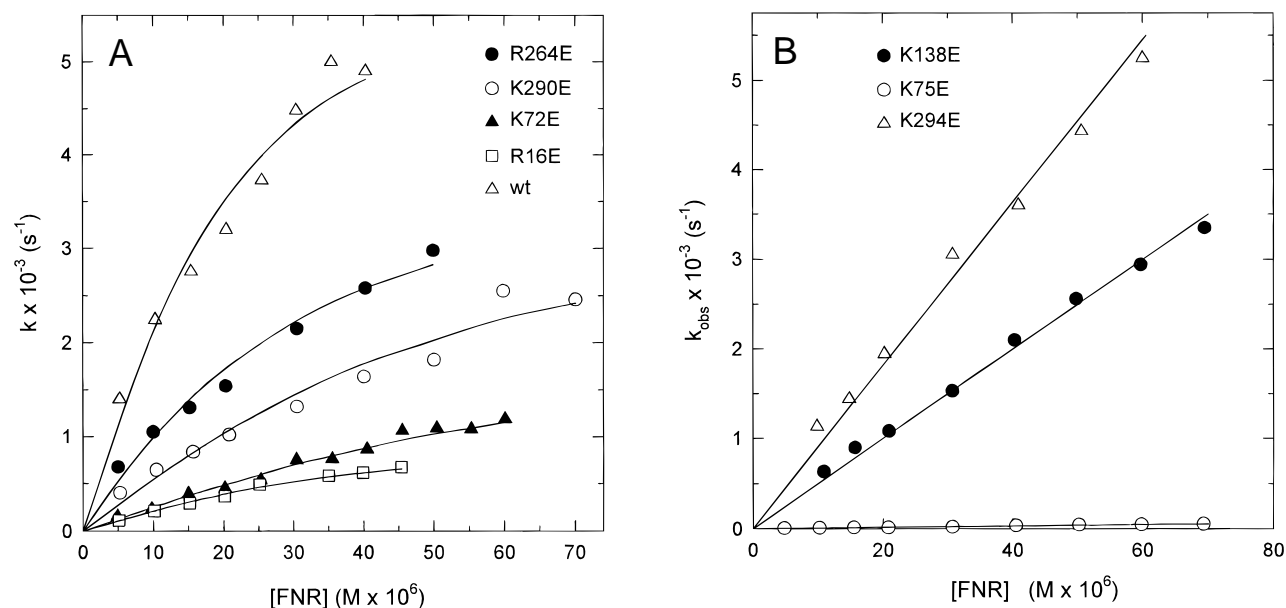


**Fig. 4.** FNR concentration dependencies for the reduction of wt and mutant FNRs by reduced Fd at 100 mM ionic strength. **A:** Wt FNR was titrated into a solution containing 30  $\mu\text{M}$  Fd. All other FNRs were titrated into solutions containing 40  $\mu\text{M}$  Fd. **B:** K75E was titrated into 30  $\mu\text{M}$  Fd; K138E and K294E were titrated into 40  $\mu\text{M}$  Fd. Solutions also contained 1mM EDTA, 0.1 mM dRf, and 4 mM potassium phosphate buffer, pH 7.0. The ionic strength was adjusted using 5 M NaCl. Note that FNR concentrations were not corrected for pre-formed complex. Monitoring wavelength was 600 nm.

**Table 2.** Electron transfer rate constants and second order rate constants for electron transfer from reduced Fd to wt and mutant FNRs at 100 mM ionic strength<sup>a</sup>

FNR	$k \times 10^{-8}$ (M <sup>-1</sup> s <sup>-1</sup> ) <sup>b</sup>	$k_{et}$ (s <sup>-1</sup> ) <sup>c</sup>
wt	2.7 ± 0.4	6,200 ± 400 <sup>d</sup>
K138E	0.50 ± 0.03	—
R264E	1.1 ± 0.1	4,200 ± 400
K290E	0.65 ± 0.10	3,800 ± 400
K294E	0.91 ± 0.02	—
R16E	0.22 ± 0.2	1,100 ± 100
K72E	0.26 ± 0.04	2,200 ± 150
K75E	0.0082 ± 0.0003	—

<sup>a</sup>Solutions contained 100 μM dRf and 1 mM EDTA in 4 mM potassium phosphate buffer, pH 7.0. The ionic strength was adjusted to 100 mM using 5 M NaCl. FNR was titrated into a solution of either 30 or 40 μM Fd.

<sup>b</sup>Second order rate constants were estimated from the initial slopes of  $k_{obs}$  vs. [FNR] curves, except for K138E, K294E, and K75E, which were measured directly from the linear plots shown in Figure 4B.

<sup>c</sup>Values obtained from the kinetic data as described in Materials and methods. The data were not corrected for the concentration of pre-formed complex.

<sup>d</sup>Data are taken from Hurley et al. (1996).

relatively electrostatically neutral region. K290 and K294 both lie on a surface exposed  $\alpha$ -helix and are charge-paired with D287 and D291, respectively. R264 is located to the left of the FAD ring and is also not charged-paired with any acidic residue, although it does lie within relatively close proximity to three acidic residues, E267, E268, and D271.

In the wt protein there are two regions of intense negative electrostatic potential. One of these, located immediately below the flavin ring, is due to the presence of E301, which is not charge-paired with any basic residue, and E139, which is charge-paired with K297. However, charge-pairing does not completely eliminate the negative potential of this latter glutamate residue. A second region of negative potential is located to the left of the flavin ring and is due to the presence of E267, E268, and D271, which are not charged-paired with any basic groups.

**Table 3.** Environments of mutated residues in FNR

Residue	Distance from dimethylbenzene ring of FAD (Å) <sup>a</sup>	Charge pairing
K138	15.6	No, but adjacent to E139
R264	6.2	No, but next to acidic patch (E267/ E268/D271)
K290	23.3	Paired with D287
K294	22.1	Paired with D291
R16	15.8	No, in neutral environment
K72	18.6	No, but close to D68/E74
K75	12.9	No, but close to D68/E74

<sup>a</sup>The distance was measured from NZ of lysines and NH1 of arginines to both CM7 and CM8 of the isoalloxazine ring of the FAD, and the shorter of these two distances is reported.

Fd is a highly acidic protein, having a net charge of  $-14$  and, as noted above, considerable experimental evidence exists for interactions between positive charges on FNR and negative charges on Fd. The kinetic results described above have shown that the FNR mutants R16E, K72E and particularly K75E have substantially weakened binding to Fd<sub>ox</sub> and lower rates of et with Fd<sub>red</sub>, whereas K138E, K264E, K290E, and K294E were only minimally affected. This correlates well with the predominantly positive potential located in the region of the former three residues and the larger degree of negative potential localized near the latter four residues. It would appear then that the region of the FNR surface, which includes K75, K72, and R16, is the most influential in controlling the binding affinity of Fd and the magnitude of the et rate constant. Charge-reversal mutations in these residues produce substantial alterations in the surface electrostatic potential. Similar charge-reversal mutations in the region corresponding to the left side of the FAD (R264E, K290E, or K294E), where there is already a substantial amount of negative potential, produced only a small increase in the predominantly negative potential of this portion of the molecule (Fig. 5) and thus would be expected to affect the binding of Fd to only a relatively small extent. K138 is adjacent to E139, is deeper in the cavity, and is close to the large area of negative potential below the FAD due to E139 and E301. Thus, similar to the R264E, K290E, and K294E mutations, placing additional negative potential at this position produces binding and kinetic parameters, which are very similar to those of the K264E, K290E, and K294E mutants (Table 1).

As noted above, the present studies corroborate recent steady-state kinetic results (Schmitz et al., 1998) with analogous mutations in *Anabaena* 7119 FNR in a ferredoxin-dependent NADP<sup>+</sup> photoreduction assay, in which R16E, K72E, and K75E had highly diminished activities, whereas K138E, R164E, K290E, and K294E had activities much like wt FNR. It is interesting to note that all of the mutants were shown to have highly decreased activity in a ferredoxin-dependent cytochrome *c* reduction assay, and all showed minimal reductions in activity in a DCPIP diaphorase assay (Schmitz et al., 1998). Presumably, this is due to the fact that the latter two assays are quite different from the physiological reaction between FNR and Fd, which occurs in the photosynthetic electron transport chain.

### Conclusions

The present studies were designed to explore the involvement of basic surface residues on FNR located close to the exposed FAD cofactor in the et interaction of FNR with Fd. At 12 mM ionic strength, measurements of the binding constants for the oxidized proteins indicate that K72E and R16E bind Fd<sub>ox</sub> much less tightly than does wt FNR and that binding of K75E was not measurable. The kinetic experiments at 100 mM ionic strength reveal that R16E and K72E also exhibit weakened binding to Fd<sub>red</sub>, and it can again be inferred from the results that K75E binds still more weakly. All of these three mutants exhibit highly impaired et reaction kinetics with reduced Fd. In contrast, four other charge-reversal mutants, K138E, R264E, K290E, and K294E, exhibit moderate to no impairment of et reactivity. As revealed by calculated electrostatic potential surface maps of wt and the mutant FNRs, the former three mutation sites are located in a region that is predominantly electrostatically neutral, whereas the latter four mutations are located in a region of high negative potential. We conclude that, although all of the residues mutated in this study are involved

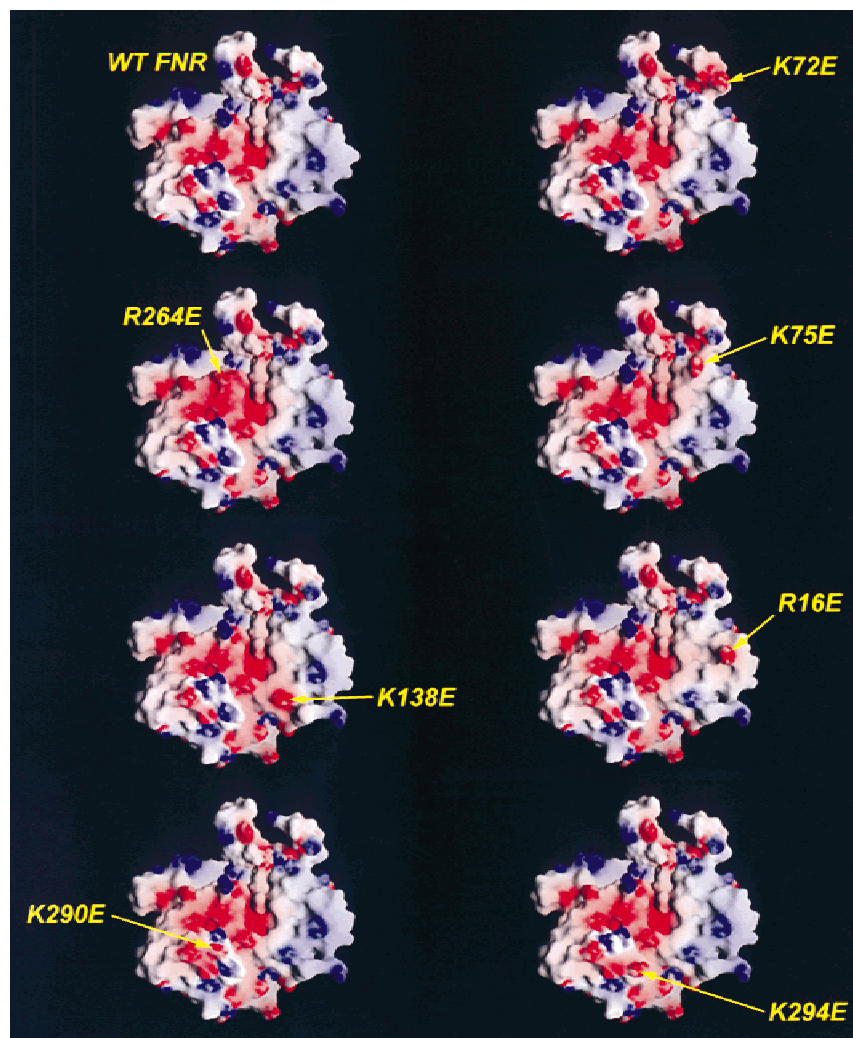


**Fig. 5.** Molecular models obtained using GRASP of wt and mutant *Anabaena* FNRs showing their electrostatic surface potentials (calculated using DELPHI). Positive potential is shown in blue, and negative potential is shown in red. Coordinates for this figure are from the Brookhaven Protein Data Bank (file code = 1QUE). Potentials were calculated as described in the text.

in binding ferredoxin during et, K75 appears to be the most important, with R16 and K72 being somewhat less so. It is possible that the charge-reversal mutations of the latter three residues repel the negatively-charged ferredoxin from its optimal docking position on FNR, resulting in both weakened binding and nonoptimal orientation for et. Adding additional negative charge to the region containing the other four basic residues produces only minimal effects on binding and protein–protein orientation during et. Mutagenesis and kinetic studies are continuing on this protein pair, with the goal of obtaining sufficient experimental information to allow a docking model of the two proteins to be established. Since hydrophobic interactions also appear to be involved in complex formation (Hurley et al., 1993, 1996; Jelesarov & Bosshard, 1994), experiments are underway to explore this aspect of complex formation and stabilization.

#### Acknowledgments

This work was supported in part by grants from the National Institutes of Health (DK15057 to G.T.) and from Comisión Interministerial de Ciencia y Tecnología (BIO97-0912CO2-01 to C.G.-M.).

#### References

- Alam J, Whitaker RA, Krogman DW, Curtis SE. 1986. Isolation and sequence of the gene for ferredoxin I from the cyanobacterium *Anabaena* sp. strain PCC 7120. *J Bacteriol* 168:1265–1271.
- Aliverti A, Corrado ME, Zanetti G. 1994. Involvement of lysine-88 of spinach ferredoxin-NADP<sup>+</sup> reductase in the interaction with ferredoxin. *FEBS Lett* 343:247–250.
- Aliverti A, Deng Z, Ravasi D, Piubelli L, Karplus PA, Zanetti G. 1998. Probing the function of the invariant glutamyl residue 312 in spinach ferredoxin:NADP<sup>+</sup> reductase. *J Biol Chem* 273:34008–34015.
- Bhattacharyya AK, Tollin G, Davis M, Edmondson DE. 1983. Laser flash photolysis studies of intramolecular electron transfer in milk xanthine oxidase. *Biochemistry* 22:5270–5279.
- Böhme H, Haselkorn R. 1989. Expression of *Anabaena* ferredoxin genes in *Escherichia coli*. *Plant Mol Biol* 12:667–672.
- De Pascalis AR, Jelesarov I, Ackermann F, Koppenol WH, Hirasawa M, Knaff DB, Bosshard HR. 1993. Binding of ferredoxin to ferredoxin:NADP<sup>+</sup> reductase: The role of carboxyl groups, electrostatic surface potential, and molecular dipole moment. *Protein Sci* 2:1126–1135.
- Fillat MF, Borrias WE, Weisbeek PJ. 1990. Cloning of the ferredoxin-NADP<sup>+</sup>-oxidoreductase gene and overexpression of a synthetic flavodoxin gene from the cyanobacteria *Anabaena* PCC 7119. In: Curti B, Ronchi S, Zanetti G, eds. *Flavins and flavoproteins 1990*. Berlin: Walter de Gruyter & Co. pp 445–448.
- Fillat MF, Pacheco ML, Peleato ML, Gómez-Moreno C. 1994. Overexpression

- of ferredoxin-NADP<sup>+</sup> reductase from *Anabaena* sp. PCC 7119 in *E. coli*. In: Yagi K, ed. *Flavins and flavoproteins 1993*. Berlin: Walter de Gruyter & Co. pp 447–450.
- Foust GP, Mayhew SG, Massey V. 1969. Complex formation between ferredoxin triphosphopyridine nucleotide reductase and electron transfer proteins. *J Biol Chem* 244:964–970.
- Fukuyama K, Ueki N, Nakamura H, Tsukahara T, Matsubara H. 1995. Tertiary structure of [2Fe-2S] ferredoxin from *Spirulina platensis* refined at 2.5 Å resolution: Structural comparisons of plant-type ferredoxins and an electrostatic potential analysis. *J Biochem* 117:1017–1023.
- Gómez-Moreno C, Martínez-Júlvez M, Fillat MF, Hurley JK, Tollin G. 1995. Molecular recognition in electron transfer proteins. In: Mathis P, ed. *Photosynthesis: From light to biosphere*, Vol. II, The Netherlands: Academic Press Publishers. pp 627–632.
- Holden HM, Jacobson BL, Hurley JK, Tollin G, Oh B-H, Skjeldal L, Chae YK, Cheng H, Xia B, Markley JL. 1994. Structure-function studies of [2Fe-2S] ferredoxins. *J Bioenerg Biomembr* 26:67–88.
- Hurley JK, Fillat MF, Gómez-Moreno C, Tollin G. 1995. Structure-function relationships in the ferredoxin/ferredoxin:NADP<sup>+</sup> reductase system from *Anabaena*. *Biochimie* 77:539–548.
- Hurley JK, Fillat MF, Gómez-Moreno C, Tollin G. 1996. Electrostatic and hydrophobic interactions during complex formation and electron transfer in the ferredoxin/ferredoxin:NADP<sup>+</sup> reductase system from *Anabaena*. *J Am Chem Soc* 118:5526–5531.
- Hurley JK, Salamon Z, Meyer TE, Fitch JC, Cusanovich MA, Markley JL, Cheng H, Xia B, Chae YK, Medina M, Gómez-Moreno C, Tollin G. 1993. Amino acid residues in *Anabaena* ferredoxin crucial to interaction with ferredoxin-NADP<sup>+</sup> reductase: Site-directed mutagenesis and laser flash photolysis. *Biochemistry* 32:9346–9354.
- Hurley JK, Weber-Main AM, Stankovich MT, Benning MM, Thoden JB, Vanhook JL, Holden HM, Chae YK, Xia B, Cheng H, Markley JL, Martínez-Júlvez M, Gómez-Moreno C, Schmeits JL, Tollin G. 1997a. Structure-function relationships in *Anabaena* ferredoxin: Correlations between X-ray crystal structures, reduction potentials, and rate constants for electron transfer to ferredoxin:NADP<sup>+</sup> reductase for site-specific ferredoxin mutants. *Biochemistry* 36:11100–11117.
- Hurley JK, Weber-Main AM, Hodges AE, Stankovich MT, Benning MM, Holden HM, Cheng H, Xia B, Markley JL, Genzor C, Gómez-Moreno C, Hafezi R, Tollin G. 1997b. Iron-sulfur cluster cysteine-to-serine mutants of *Anabaena* [2Fe-2S] ferredoxin exhibit unexpected redox properties and are competent in electron transfer to ferredoxin:NADP<sup>+</sup> reductase. *Biochemistry* 36:15109–15117.
- Jelesarov I, Bosshard HR. 1994. Thermodynamics of ferredoxin binding to ferredoxin:NADP<sup>+</sup> reductase and the role of water at the complex interface. *Biochemistry* 33:13321–13328.
- Jelesarov I, De Pascalis AR, Koppenol WH, Hirasawa M, Knaff DB, Bosshard HR. 1993. Ferredoxin binding site on ferredoxin:NADP<sup>+</sup> reductase. Differential chemical modification of free and ferredoxin-bound enzyme. *Eur J Biochem* 216:57–66.
- Karplus PA. 1991. Structure/function of spinach ferredoxin:NADP<sup>+</sup> oxidoreductase. In: Curti B, Ronchi S, Zanetti G, eds. *Flavins and flavoproteins 1990*. Berlin: Walter de Gruyter & Co. pp 449–455.
- Karplus PA, Bruns CM. 1994. Structure-function relationships for ferredoxin reductase. *J Bioenerg Biomembr* 26:89–99.
- Karplus PA, Daniels MJ, Herriot JR. 1991. Atomic structure of ferredoxin-NADP<sup>+</sup> reductase: Prototype for a structurally novel flavoenzyme family. *Science* 251:60–66.
- Knaff DB. 1996. Ferredoxin and ferredoxin-dependent enzymes. In: Ort DR, Yocum CF, eds. *Oxygenic photosynthesis: The light reactions*. Dordrecht: Kluwer Academic Publishers. pp 333–361.
- Knaff DB, Hirasawa M. 1991. Ferredoxin-dependent chloroplast enzymes. *Biochim Biophys Acta* 1056:93–125.
- Martínez-Júlvez M, Medina M, Hurley JK, Hafezi R, Brodie TB, Tollin G, Gómez-Moreno C. 1998. Lys 75 of *Anabaena* ferredoxin-NADP<sup>+</sup> reductase is a critical residue for binding ferredoxin and flavodoxin during electron transfer. *Biochemistry* 37:13604–13613.
- Medina M, Martínez-Júlvez M, Hurley JK, Tollin G, Gómez-Moreno C. 1998. Involvement of glutamic acid 301 in the catalytic mechanism of ferredoxin-NADP<sup>+</sup> reductase from *Anabaena* PCC 7119. *Biochemistry* 37:2715–2728.
- Medina M, Méndez E, Gómez-Moreno C. 1992a. Lysine residues on ferredoxin-NADP<sup>+</sup> reductase from *Anabaena* sp. 7119 involved in substrate binding. *FEBS Lett* 298:25–28.
- Medina M, Méndez E, Gómez-Moreno C. 1992b. Identification of arginyl residues involved in the binding of ferredoxin-NADP<sup>+</sup> reductase from *Anabaena* sp. 7119 to its substrates. *Arch Biochem Biophys* 299:281–286.
- Nicholls A, Sharp K, Honig B. 1991. Protein folding and association: Insights from the interface and thermodynamic properties of hydrocarbons. *Proteins Struct Funct Genet* 11:281–296.
- Przysocki CT, Bhattacharyya AK, Tollin G, Cusanovich MA. 1985. Kinetics of reduction of *Clostridium pasteurianum* rubredoxin by laser photoreduced spinach ferredoxin:NADP<sup>+</sup> reductase and free flavins. *J Biol Chem* 260:1452–1458.
- Rypniewski WR, Breiter DR, Benning MM, Wesenberg G, Oh B-H, Markley JL, Rayment I, Holden HM. 1991. Crystallization and structure determination to 2.5 Å resolution of the oxidized [2Fe-2S] ferredoxin isolated from *Anabaena* 7120. *Biochemistry* 30:4126–4131.
- Sancho J, Gómez-Moreno C. 1991. Interactions of ferredoxin-NADP<sup>+</sup> reductase from *Anabaena* with its substrates. *Arch Biochem Biophys* 288:231–238.
- Schmitz S, Martínez-Júlvez M, Gómez-Moreno C, Böhme H. 1998. Interaction of positively charged amino acid residues of recombinant, cyanobacterial ferredoxin:NADP<sup>+</sup> reductase with ferredoxin probed by site-directed mutagenesis. *Biochim Biophys Acta* 1363:85–93.
- Serre L, Vellieux FMD, Medina M, Gómez-Moreno C, Fontecilla-Camps JC, Frey M. 1996. X-ray structure of the ferredoxin:NADP<sup>+</sup> reductase from the cyanobacterium *Anabaena* PCC 7119 at 1.8 Å resolution, and the crystallographic studies of NADP<sup>+</sup> binding at 2.25 Å resolution. *J Mol Biol* 263:20–39.
- Simonsen RP, Tollin G. 1983. Transient kinetics of redox reactions of flavodoxin: Effects of chemical modification of the flavin mononucleotide prosthetic group on the dynamics of intermediate complex formation and electron transfer. *Biochemistry* 22:3008–3016.
- Simonsen RP, Weber PC, Salemm FR, Tollin G. 1982. Transient kinetics of electron transfer reactions of flavodoxin: Ionic strength dependence of semiquinone oxidation by cytochrome *c*, ferricyanide, and ferric ethylenediaminetetraacetic acid and computer modeling of reaction complexes. *Biochemistry* 21:6366–6375.
- Tollin G. 1995. Use of flavin photochemistry to probe intraprotein and interprotein electron transfer mechanisms. *J Bioenerg Biomembr* 27:303–309.
- Tollin G, Hazzard JT. 1991. Intra- and intermolecular electron transfer processes in redox proteins. *Arch Biochem Biophys* 287:1–7.
- Tollin G, Hurley JK, Hazzard JT, Meyer T. 1993. Use of laser flash photolysis time-resolved spectrophotometry to investigate interprotein and intraprotein electron transfer mechanisms. *Biophys Chem* 48:259–279.
- Zanetti G, Aliverti A. 1991. Ferredoxin:NADP<sup>+</sup> oxidoreductase. In: Müller F, ed. *Chemical and biochemical flavoenzymes*, Vol. II. Boca Raton, Florida: CRC Press. pp 305–315.
- Zanetti G, Morelli D, Ronchi S, Negri A, Aliverti A, Curti B. 1988. Structural studies on the interaction between ferredoxin and ferredoxin:NADP<sup>+</sup> reductase. *Biochemistry* 27:3753–3759.